

FULL PAPER

Open Access



In situ stress magnitude and rock strength in the Nankai accretionary complex: a novel approach using paired constraints from downhole data in two wells

K. A. Huffman^{1*}, D. M. Saffer¹ and B. Dugan²

Abstract

We present a method to simultaneously constrain both far-field horizontal stress magnitudes (S_{hmin} and S_{Hmax}) and in situ rock unconfined compressive strength (UCS), using geophysical logging data from two boreholes located 70 m apart that access the uppermost accretionary prism of the Nankai subduction zone. The boreholes sample the same sediments and are affected by the same tectonic stress field, but were drilled with different annular pressures, thus providing a unique opportunity to refine estimates of both in situ stress magnitudes and rock strength. We develop a forward model to predict the angular width of compressional wellbore failures (borehole breakouts), and identify combinations of S_{Hmax} and UCS that best match breakout widths observed in resistivity images from the two boreholes. The method requires knowledge of S_{hmin} , which is defined by leak-off tests conducted during drilling. Our results define a normal to strike-slip stress regime from 900 to 1386 m below seafloor, consistent with observations from seismic and core data. Our analysis also suggests that in situ values of UCS are generally slightly lower than commonly assumed on the basis of published empirical relations between UCS and P-wave velocity.

Keywords: Nankai Trough, In situ stress, Unconfined compressive strength, Borehole breakout, IODP

Introduction

Understanding in situ tectonic stress and rock strength at seismically active margins is important for characterizing fault strength and failure mechanics, yet direct measurements of these quantities are rare. Hydrofracturing and leak-off tests are commonly employed in drilling to measure the minimum principal stress, but provide information only at specific depths and are costly (e.g., Bell 1990; Engelder 1993; Lin et al. 2008; Saffer et al. 2010; Hung et al. 2009). The direct measurement of maximum horizontal stress magnitude is more difficult, and few tools for this exist (e.g., Moran et al. 1993). As a result, indirect approaches have been widely used to

estimate in situ horizontal stress orientation and magnitude from wellbore failures and from fault or fracture orientations measured in borehole logging data (e.g., Moos and Zoback 1990; Zoback and Healy 1992; Brudy et al. 1997; Zoback 2007; Chang et al. 2010; Ito et al. 2013; Lin et al. 2015) or from anelastic strain recovery measurements on core samples (e.g., Amadei and Stephansson 1997; Lin et al. 2006; Byrne et al. 2009). Similarly, in situ strength must be inferred indirectly from downhole drilling parameters (e.g., Kerker et al. 2014) or defined from laboratory measurements (e.g., Horsrud 2001; Song et al. 2011; Chang et al. 2006). Laboratory measurements require core samples, are time-consuming, and must be upscaled to apply them in the field.

Recent work at subduction margins, including the Integrated Ocean Drilling Program (IODP) Nankai Trough Subduction Zone Experiment (NanTroSEIZE) (Fig. 1), has used the width of compressional wellbore breakouts to estimate the magnitude of the maximum and

*Correspondence: katelyn.huffman@gmail.com

¹ Department of Geosciences and Center for Geofluids, Geomechanics, and Geohazards, The Pennsylvania State University, University Park, PA 16802, USA

Full list of author information is available at the end of the article

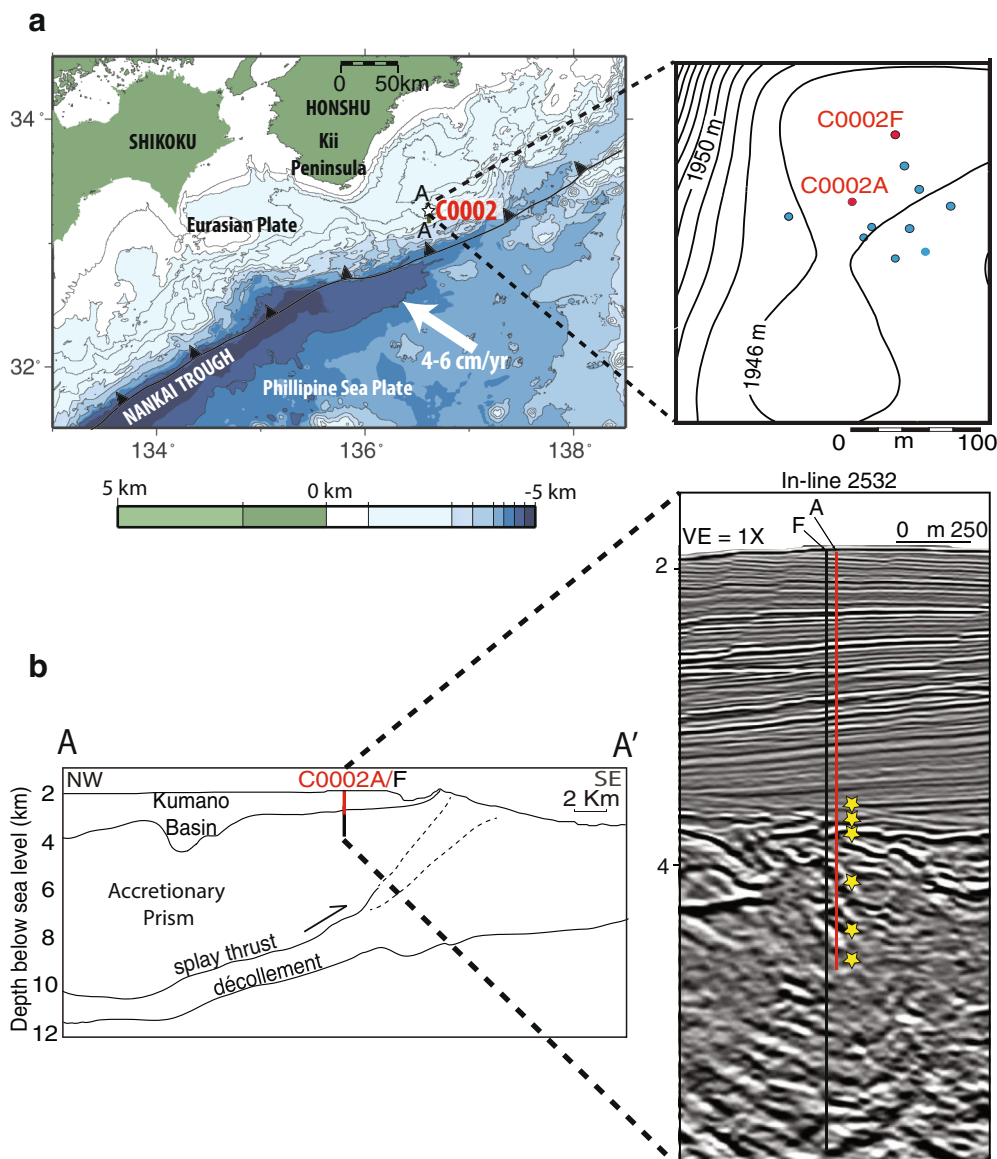
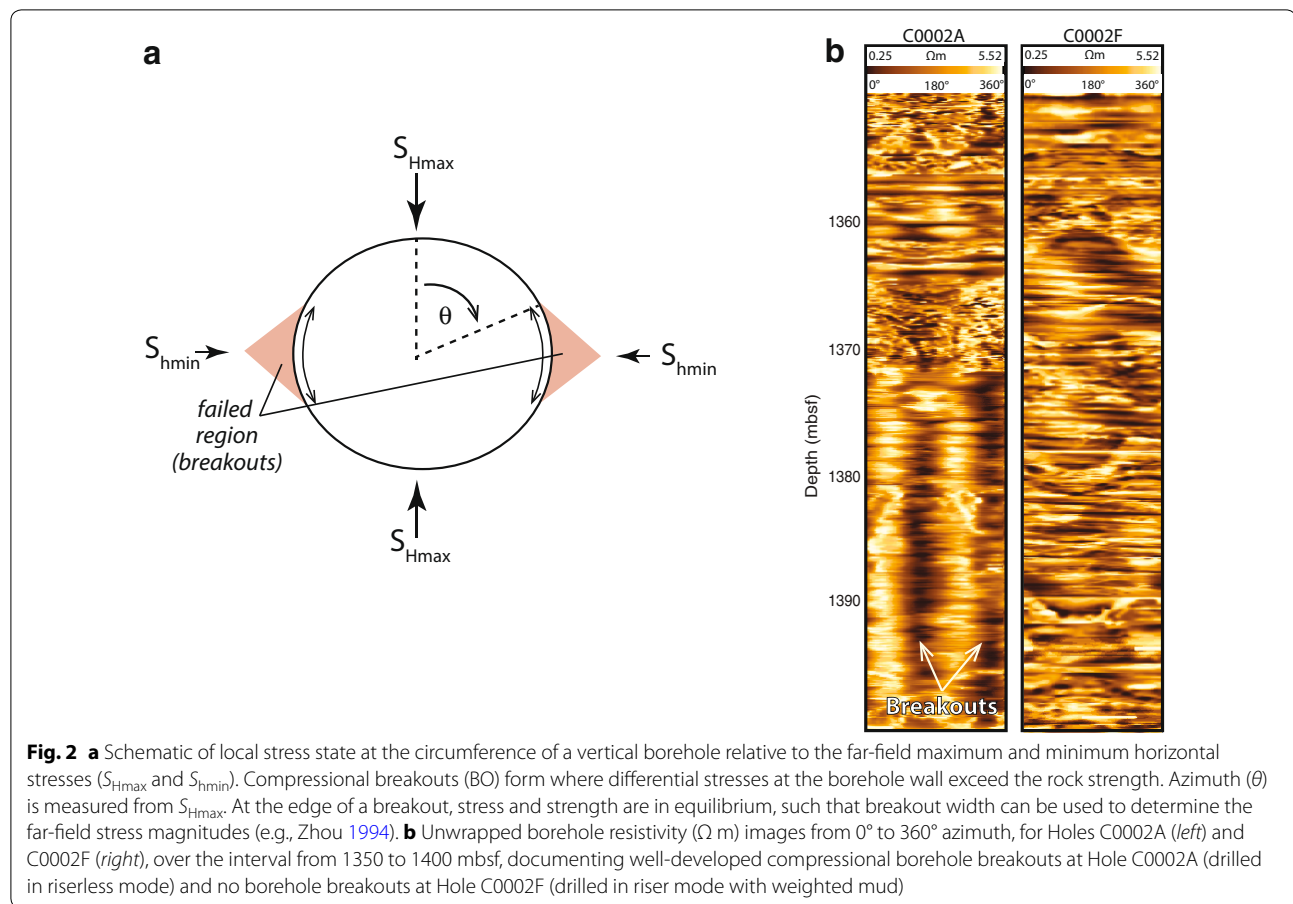


Fig. 1 **a** Map of Nankai Trough showing the location of IODP Site C0002, ~30 km from the trench. Multiple boreholes were drilled at Site C0002 (blue and red circles). We focus on Holes C0002A and C0002F (red circles), located 70 m apart. **b** Seismic line drawing showing location of Site C0002 relative to major structural features (shown schematically). Seismic image shows detailed view of the rock volume intersected by the two boreholes. VE = vertical exaggeration. Yellow stars represent the depths of our analysis

minimum horizontal principal stresses (S_{Hmax} and S_{Hmin}) (e.g., Chang et al. 2010; Lin et al. 2013). Far-field stress is distorted in a predictable way at the circular free surface introduced by borehole excavation, such that the principal stresses are normal and tangential to the borehole wall, with the latter varying as a function of azimuth (e.g., Kirsch 1898). Breakouts form only at azimuths around the borehole where local differential stress at the borehole wall exceeds the rock's failure criterion (Fig. 2a) (Zoback 2007). Thus, if rock strength is known, breakout

widths measured by downhole logging can provide an indication of the far-field principal stress magnitudes (e.g., Moos and Zoback 1990; Chang et al. 2010). However, large uncertainties in assumed or estimated rock strength (e.g., unconfined compressive strength, UCS; friction coefficient, μ) lead to large uncertainties in the estimated stress magnitudes, because there is a direct trade-off between the two in determining the stresses required for rock failure (Huffman and Saffer 2016). In the absence of direct laboratory measurements, UCS is



commonly assumed or estimated from P-wave velocity (V_p), using empirical fits for various rock types (e.g., Lal 1999; Horsrud 2001; Chang et al. 2006, 2010). However, it is unclear whether these empirical relations, even for shale, are representative of unlithified mudstones with porosity of 10–20 % which are typical of the upper few km of the subsurface, and for which few laboratory data are available.

The availability of downhole logging data from two adjacent (offset 70 m; Fig. 1) boreholes at Integrated Ocean Drilling Program (IODP) Site C0002 presents a rare opportunity to simultaneously constrain both rock strength and stress magnitudes through an in situ experiment. This differs from previous analyses, in which UCS has been assumed (or estimated from V_p) in order to then compute a range of S_{Hmax} consistent with observed wellbore failures. The two holes were drilled with the same diameter into the same sedimentary sequences and were affected by the same far-field stresses, but were drilled with different downhole annular pressures (APRS). Here, we combine observations of wellbore breakouts at the two sites to place bounds on both the in situ horizontal stress magnitudes and UCS.

Although previous work has focused on the in situ stress magnitudes (e.g., Chang et al. 2010; Lin et al. 2013; Yamada and Shibamura 2015), the use of two holes allows us, for the first time, to concurrently constrain formation strength in situ. To accomplish this, we develop a forward model to predict breakout width in each borehole using direct measurements of APRS from measurement while drilling (MWD) tools and of S_{hmin} from leak-off tests. We then find combinations of S_{Hmax} and UCS that best match the paired observations of borehole breakouts measured in resistivity images from the two holes. From this, we define a vertical profile of in situ stress and strength, which constrains the full stress tensor in the lowermost Kumano forearc basin and uppermost accretionary prism (Fig. 1). We discuss the implications of these in situ stress magnitudes and UCS values for the faulting regime and for empirical relations between rock strength and P-wave velocity that are commonly used to constrain stress magnitudes using borehole breakouts.

Geologic setting and background

The Nankai Trough is formed by northwestward subduction of the Philippine Sea Plate (PSP) beneath the

Eurasian Plate offshore southern Honshu at $\sim 4.1\text{--}6.5$ cm/year (Fig. 1a) (Seno et al. 1993; Miyazaki and Heki 2001). The subduction zone is typified by $M_w > 8$ earthquakes that recur every $\sim 100\text{--}200$ years (Ando 1975). As the PSP subducts, part of the incoming sedimentary succession is offscraped at the trench, forming a ~ 100 -km-wide accretionary prism (Fig. 1) (e.g., Moore et al. 1990). Major research initiatives to study the Nankai Trough include active and passive source seismic surveys (e.g., Moore et al. 1990, 2009), drilling, and analysis of associated core, cuttings, and geophysical data (e.g., Karig et al. 1975; Moore et al. 2001; Tobin et al. 2009). Scientific drilling in the Nankai Trough has included Ocean Drilling Program (ODP) Legs 131, 190, and 196 (Hill et al. 1993; Moore et al. 2001; Mikada et al. 2002) offshore of Shikoku Island, and several IODP Expeditions offshore the Kii Peninsula as part of the NanTroSEIZE experiment (Expeditions 314–316, 319, 322, 326, 332–333, 338, and 348) (Kinoshita et al. 2009; Tobin et al. 2009, 2015; Saffer et al. 2010; Saito et al. 2010; Kopf et al. 2011; Henry et al. 2012; Moore et al. 2013). These efforts have provided important information about the plate boundary and outer forearc, including its overall structure, fault zone properties, and hydrogeology.

We focus on IODP Site C0002, located approximately 30-km landward of the trench along the NanTroSEIZE drilling transect, above the inferred seismogenic portion of the plate boundary (Fig. 1) (Tobin et al. 2015; Moore et al. 2013). Operations at Site C0002 included the drilling of multiple holes (Fig. 1). We analyze data from Holes C0002A and C0002F, two vertical boreholes separated by 70 m in map view (Fig. 1). The boreholes penetrated ~ 918 m of the Kumano forearc basin fill, composed of Pliocene-to-Pleistocene mudstones and turbidites, and into the uppermost several hundred meters of the underlying accretionary wedge, composed of Miocene silty claystones with lesser amounts of sandstone and sandy siltstone (Ashi et al. 2008, 2009; Moore et al. 2013). Holes C0002F and C0002A provide data with overlapping coverage from 872 to 1401 meters below the seafloor (mbsf).

During Expedition 314 in 2007, Hole C0002A was drilled as a dedicated logging-while-drilling (LWD) hole and penetrated from the seafloor to 1401 mbsf in a riserless drilling mode (Tobin et al. 2015). In riserless drilling, the annular wellbore pressure is not actively controlled, but is governed by the hydrostatic pressure plus any additional pressure associated with cuttings in the well and dynamic circulation during drilling. Azimuthal electrical resistivity images from Hole C0002A document well-developed and continuous breakouts throughout the hole, oriented at azimuths of $135^\circ\text{--}315^\circ \pm 45^\circ$ (Fig. 2b). This indicates that S_{Hmax} is oriented at $\sim 45^\circ\text{--}225^\circ$, sub-parallel to the trench (Lin et al. 2010; Chang et al. 2010).

The observed breakout angular widths range from 20 to 140° , with an average of 70° (Ashi et al. 2009). There is little change in S_{Hmax} orientation from the Kumano basin into the accretionary prism below (Lin et al. 2010; Chang et al. 2010). Previous analyses of the breakout widths to estimate far-field stress magnitudes suggest a normal faulting regime (overburden stress or $S_v = \sigma_1$) within the Kumano basin (<918 mbsf), which transitions to a strike-slip or thrust regime (maximum horizontal stress or $S_{Hmax} = \sigma_1$) in the accretionary prism below (>918 mbsf) (Chang et al. 2010).

Hole C0002F was drilled to 872 mbsf in riserless drilling mode in 2010 with a limited set of LWD measurement tools (Expedition 326 Scientists 2011). It was deepened to 2006 mbsf in a riser drilling mode in 2012 (Strasser et al. 2014) and to 3058.5 mbsf in 2014 (Tobin et al. 2015) with a full suite of LWD tools. In riser drilling, annular pressure is controlled by the use of weighted drilling mud and return circulation in a riser pipe that connects the borehole to the drilling platform at the sea surface through the water column. For Expedition 338, mud with a density of 1100 kg/m^3 was used. Leak-off tests (LOTs) conducted in Hole C0002F at 874 and 1954.5 mbsf indicate a minimum principal stress, defined from leak-off pressures (e.g., Zoback 2007), of 12.6 and 33.6 MPa, respectively, at these depths (pressures are referenced to zero at the seafloor) (Strasser et al. 2014; Tobin et al. 2015). In both cases, the leak-off pressures are less than the total vertical stress (S_v), indicating that S_{Hmin} is the minimum principal stress. This indicates that the stress state lies in either a normal or strike-slip faulting regime throughout the section, which is broadly consistent with observations of abundant normal faults in the Kumano basin in seismic reflection data (e.g., Sacks et al. 2013) and with previous estimates of stress magnitudes from wellbore breakouts (Chang et al. 2010). In the underlying accretionary prism, seismic data document thrust splay faults that were active until ~ 0.4 Ma, but these thrust faults do not disrupt younger sediments (Boston et al. 2016). If these structures remain active at rates less than resolvable by the seismic data or are near-failure, the stress state at depth must transition to a thrust faulting regime (i.e., S_v is the minimum principal stress, and S_{Hmax} is the maximum principal stress). Such a transition is also expected at greater depth closer to the active plate boundary megathrust.

Azimuthal resistivity images from Hole C0002F (Expedition 338) indicate few breakouts (Fig. 2b); the lack of breakouts was due to hole stabilization by downhole pressure control during riser drilling. Only three breakouts were documented in Hole C0002F; they were at 916, 1617, and 1861.5 mbsf, and they range from 34° to 63° in angular width (Strasser et al. 2014). Comparison

of borehole data and interpretations in the overlapping interval for the two holes reveals six depth locations where there are clear breakouts in Hole C0002A but not in Hole C0002F (Table 1). At 916 mbsf (in the overlapping portion of Holes C0002A and F) clear breakouts were not observed in Hole C0002A due to bad data coverage. Bad data coverage could be due to large breakouts that span the majority of the borehole circumference and degrade images or due to operational issues.

Methods

Our approach identifies combinations of UCS and far-field horizontal stress magnitude that are consistent with observed breakout widths at the two adjacent boreholes (i.e., measured breakout widths where they are documented, and zero width where there are no breakouts). We use a forward model to define expected breakout widths for a wide range of boundary conditions and rock properties and then identify the combinations of far-field stress magnitude and UCS that best reproduce measured breakout widths at Hole C0002A and the lack of breakouts at Hole C0002F, which were drilled with different annular pressures. We report all pressures and stresses referenced to zero at the seafloor.

To predict breakout widths, we use the Kirsch (1898) equations to define the local principal stresses at the circumference of the wellbore, in combination with the modified Wiebols–Cook (MWC) failure criterion (Zhou 1994; Chang et al. 2010), a brittle/frictional failure criterion that incorporates the effects of the intermediate principal stress on rock strength. The underlying assumption in this approach is that at the edge of a breakout, differential stress is balanced with the rock strength (Fig. 2a) (Moos and Zoback 1990; Zoback 2007). The MWC failure criterion, which constrains σ_1 , σ_2 , and σ_3 at the edge of breakout, depends on UCS and the coefficient of internal friction (μ). The stress redistribution as a function of

borehole azimuth (θ) at the free surface of the wellbore requires assumptions or measurements of overburden stress (S_v), annular pressure (APRS), maximum horizontal stress (S_{Hmax}), minimum horizontal stress (S_{Hmin}), formation pore pressure (P_p), and Poisson's ratio (ν) (Table 1). The resulting principal stresses are given by (Kirsch 1898; Zoback 2007):

$$\sigma_{\theta\theta} = \sigma_1 = S_{Hmax} + S_{Hmin} - 2(S_{Hmax} - S_{Hmin}) \cos 2\theta - P_p - APRS \quad (1a)$$

$$\sigma_{zz} = \sigma_2 = S_v - 2\nu(S_{Hmax} - S_{Hmin}) \cos 2\theta - P_p \quad (1b)$$

$$\sigma_{rr} = \sigma_3 = APRS - P_p \quad (1c)$$

where $\sigma_{\theta\theta}$ is the tangential effective stress (acting parallel to the borehole wall), σ_{zz} is the vertical effective stress, and σ_{rr} is the radial effective stress (acting perpendicular to the borehole wall). Substituting the above equations for stress at the wellbore into the MWC failure criterion allows for prediction of breakout width in forward models.

Because breakout widths are strongly sensitive to the values of S_{Hmax} and UCS, and because these two quantities are the least constrained of the parameters that affect breakout formation, we treat them as unknowns and specify values for the other parameters on the basis of existing data. In previous studies of wellbore breakouts in the Nankai accretionary complex, a friction coefficient of 0.6 was assumed, but few direct laboratory tests were available to constrain this. Triaxial tests on core samples of Miocene mudstones from Sites 1174 (outboard of the trench offshore Shikoku Island) and C0002 indicate values of $\mu = 0.48$ (Olcott and Saffer 2013). Based on these data, we assume $\mu = 0.48$ in our analysis, but also explore the effect of this choice by considering a case where $\mu = 0.6$ for an example at 1150 mbsf. We assume Poisson's ratio is 0.45, following Peacock et al. (2010) and

Table 1 Key parameters at the depths of breakout occurrence in Hole C0002A within the overlapping interval for the two holes

Depth (mbsf)	S_{Hmin} (MPa)	S_v (MPa)	P_p (MPa)	Breakout width (°) C0002A	APRS C0002A (MPa)	APRS C0002F (MPa)	V_p (m/s)	S_{Hmax} (MPa)	UCS (MPa)
900	13.0	16.4	9.1	32	9.5	12.2	2380	17.0 ± 5.2	12.8 ± 7.2
950	13.8	17.3	9.6	6	10.2	13.1	2344	17.2 ± 5.1	12.2 ± 7.8
1000	14.8	18.2	10.1	7	10.7	13.8	2357	18.6 ± 5.1	9.3 ± 5.3
1150	17.6	20.9	11.5	110	13.0	15.3	2422	20.1 ± 3.2	6.4 ± 2.6
1300	20.4	23.9	13.1	78	14.6	17.2	2805	23.8 ± 4.7	10.2 ± 4.8
1386	22.0	25.4	13.9	100	16.5	18.3	3000	23.7 ± 2.9	5.6 ± 2.4

S_{Hmin} is determined from a gradient defined by the leak-off tests. Vertical stress (S_v), formation pore pressure (P_p), breakout width, annular pressure (APRS), and P-wave velocity (V_p) are measured, estimated, or calculated from drilling data (Tobin et al. 2015; Strasser et al. 2014). Maximum horizontal stress (S_{Hmax}) and unconfined compressive strength (UCS) are constrained by our forward modeling analyses. All stresses and pressures are referenced to zero at the seafloor. The best-fit S_{Hmax} and UCS values in are taken from the lowest residual values

Tsuji et al. (2011) from inverted P- and mode-converted S-wave velocities from active-source ocean bottom seismometers and from the time lag between P-refracted waves and PPS-converted waves from active-source ocean bottom seismometers, respectively.

We define the overburden stress (S_v) by integrating density data obtained from core samples (Ashi et al. 2009; Strasser et al. 2014). We assume that formation pore pressure (P_p) is hydrostatic based on sedimentation models for the Kumano basin, consolidation tests on core samples, and direct measurements conducted during drilling at nearby IODP Site C0009 (Guo et al. 2013; Saffer et al. 2013). Values of annular pressure (APRS) in both holes were recorded continuously during drilling (Table 1) (Ashi et al. 2009; Strasser et al. 2014). We define S_{hmin} using the results of the two LOTs, one in Hole C0002F and one in Hole C0002P. Within the Kumano basin (<918 mbsf), we fit a linear gradient from $S_{hmin} = 0$ MPa at the seafloor to $S_{hmin} = 12.6$ MPa defined by the LOT at 874 mbsf in Hole C0002F (Strasser et al. 2014). For the accretionary prism (>918 mbsf), we define a second linear gradient between the LOT at 874 mbsf and a LOT at 1954.5 mbsf, where $S_{hmin} = 33.6$ MPa in Hole C0002P (Table 1) (Tobin et al. 2015). To account for uncertainty in the leak-off tests themselves and in extrapolation along assumed linear gradients between the measurements, we consider a range of S_{hmin} of ± 2 MPa around the values defined by these gradients.

In our forward models, we evaluate a range of potential S_{Hmax} values based on the limits for frictional failure along pre-existing faults (Zoback 2007) and assuming that the principal stresses are horizontal and vertical (e.g., Chang et al. 2010). For our lower bound of S_{hmin} , this defines a range of S_{Hmax} from 11.5 to 32.2 MPa at 900 mbsf and 20.5 to 42.9 MPa at 1386 mbsf. Due to the absence of reliable data on strength of poorly lithified mudstones, we consider a broad range of possible UCS values, from 0 to 20 MPa, consistent with laboratory tests on shale (e.g., Lal 1999; Horsrud 2001).

We define goodness of fit on the basis of the minimum residual (R , in degrees) between predicted and observed angular borehole widths at the two holes and weighting the observations at the two holes equally:

$$R = |\theta_{Apred} - \theta_{Aobs}| + |\theta_{Fpred} - \theta_{Fobs}|, \quad (2)$$

where θ_{Apred} and θ_{Fpred} are the predicted breakout widths for the two boreholes from our forward model (with different annular pressures in each) and θ_{Aobs} and θ_{Fobs} are the observed breakout widths. At depths where breakouts are not observed in Hole C0002F, θ_{Fobs} is equal to zero. Any forward models that yield breakouts therefore generate a misfit to the observation, in the same manner as a misfit would arise from over- or under-predicting

breakout widths where they are observed. However, the lack of breakouts can be achieved by a wider range of UCS and S_{Hmax} than breakouts of a finite width; this is because the lack of breakouts defines only an upper bound on S_{Hmax} or a lower bound on UCS. Therefore, for any combinations of sufficiently large UCS or small S_{Hmax} , $(\theta_{Fpred} - \theta_{Fobs})$ is zero; as a result, our analysis produces a broader minimum residual in these cases.

Results and discussion

At all depths, there is a narrow range of best-fit UCS– S_{Hmax} pairs for a given value of S_{hmin} (Fig. 3). As an illustrative example of residuals at a given S_{hmin} within the range defined by LOT estimates ± 2 MPa, we show two example sets of residuals: one at 900 mbsf in the Kumano basin where $S_{hmin} = 12.9$ MPa (Fig. 3a) and one at 1150 mbsf well within the prism (>918 mbsf) where $S_{hmin} = 19.6$ MPa (Fig. 3b). Similar analyses for the six depths where breakouts are observed in Hole C0002A but not in Hole C0002F yield a depth profile of S_{Hmax} , ranging from 11.9 to 22.1 MPa at 900 mbsf to 20.8–26.6 MPa at 1386 mbsf (Table 1; Fig. 4a). The corresponding profile of best-fit in situ UCS values ranges from 5.6 to 20 MPa at 900 mbsf to 3.2–8 MPa at 1386 mbsf (Table 1; Fig. 4b). Uncertainty in S_{hmin} is the primary cause for the large ranges in both S_{Hmax} and UCS (Eq. 1; Fig. 4). In contrast, the coefficient of friction has a relatively minor effect. Varying μ from 0.48 to 0.6 results an increase in best-fit UCS and S_{Hmax} values of only ~ 1 MPa ($\sim 10\%$ of UCS and $\sim 2.5\%$ of S_{Hmax}).

Previous estimates of stress magnitude from borehole breakouts at Site C0002 were computed using rock strength values defined from empirical relationships between P-wave velocity (V_p) and UCS for shales and were formulated without constraints on S_{hmin} , which are now constrained by leak-off tests (e.g., Chang et al. 2010). These previous analyses suggested a stress state that lies in the normal faulting regime within the Kumano basin and transitions to a strike-slip or reverse faulting regime in the accretionary prism. This interpretation is broadly consistent with observations of normal faults in the Kumano basin (Sacks et al. 2013) and with major thrust splay faults within the prism (Moore et al. 2009). However, the LOTs show that at least to ~ 2000 mbsf, S_{hmin} is the least principal stress (i.e., S_{hmin} is less than S_v), limiting stresses to a normal or strike-slip regime in this depth range both at Site C0002 (Strasser et al. 2014; Tobin et al. 2015) and at Site C0009 located ~ 20 -km landward (Ito et al. 2013; Saffer et al. 2013). The inconsistency between our result and the imaging of thrust faults in the accretionary wedge could indicate that these structures are no longer active (Boston et al. 2016), that S_{Hmax} and S_{hmin} increase with depth to become the maximum

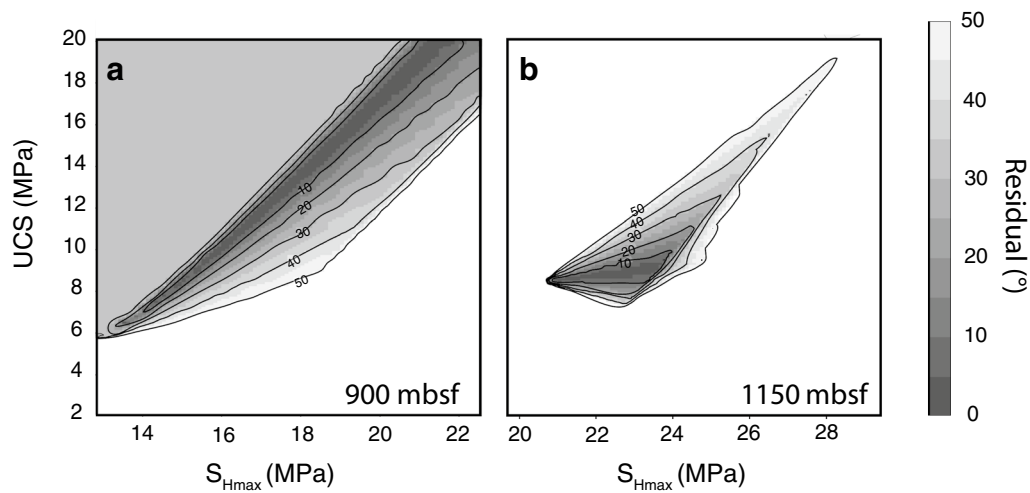


Fig. 3 Contour plots of residual of predicted versus observed breakout width for examples from 900 mbsf (a) and 1150 mbsf (b)

and intermediate principal stresses, or that the stress regime changes through the earthquake cycle and will build toward a thrust regime as strain accumulates during the interseismic period (e.g., Wang and Hu 2006). The hypothesis that horizontal stress magnitudes fluctuate during the seismic cycle is broadly consistent with temporal variations in stress interpreted from analyses of calcite crystallography in samples from the accretionary prism (Takeshita et al. 2014).

Compared to previous constraints on stress from breakouts that do not include data from two boreholes, our analysis narrows the range of S_{Hmax} to 1400 mbsf and also indicates either a normal or strike-slip faulting regime in this depth range. Uncertainties remain too large to distinguish between the two faulting regimes, because the range of S_{Hmax} we predict overlaps with S_v (Fig. 4a) and the range of S_{hmin} we consider (± 2 MPa from LOT gradients). In total, the available observations suggest that if thrust faults in the wedge are active, then the stress regime must transition to one of thrusting ($S_{hmin} > S_v$) at depths > 2000 mbsf or must evolve in time to drive thrust faulting later in the seismic cycle (e.g., Wang and Hu 2006; Sacks et al. 2013; Hardebeck 2012; Lin et al. 2013; Huffman and Saffer 2016).

The values of UCS determined from our analysis are in general agreement with, but fall slightly below, empirical relations between V_p and UCS for shale (e.g., Lal 1999; Horsrud 2001) and are in good agreement with the trend in rock strength defined by laboratory experiments on a limited set of core samples from the Nankai margin (Song et al. 2011; Olcott and Saffer 2013) (Fig. 4c). Sonic logs spanning the depth range we analyzed document V_p values that cluster near 2400 m s^{-1} (for depths 900–1150 mbsf) and $2800\text{--}3000 \text{ m s}^{-1}$

(depths 1300–1386 mbsf) (Table 1). Our forward model results indicate a range of UCS that is broadly consistent with empirical relations in the shallower zone, but lower than predicted by these relations for the deeper interval. In combination, the values of UCS defined by our analysis and by direct laboratory tests (Olcott and Saffer 2013) suggest that empirical relations between V_p and UCS for shale may overestimate rock strength slightly; this would result in an overestimate of far-field tectonic stress derived from breakout widths (e.g., Chang et al. 2010; Lin et al. 2013).

Conclusions

Quantification of in situ horizontal stress magnitudes and rock strength is challenging, typically owing to a lack of data needed to constrain models. The problem is further complicated by the fact that most methods employed to estimate in situ stress magnitudes require independent datasets to constrain rock strength. Here we address this problem by using data from two adjacent boreholes drilled with different boundary conditions (annular pressures) that sample the same volume of the shallow crust in an active tectonic setting, and where the minimum horizontal stress is measured independently by leak-off tests. Our approach simultaneously defines the best-fit in situ maximum horizontal stress magnitude (S_{Hmax}) and rock unconfined compressive strength (UCS), using a forward model of compressional borehole breakouts that is constrained by observations of wellbore failure, or lack of wellbore failure, at the two adjacent holes. This ultimately allows estimation of the full stress tensor at several depths in the Kumano forearc basin and underlying upper accretionary prism. We find that S_{Hmax} ranges from 11.9 to 22.2 MPa at 900 mbsf to

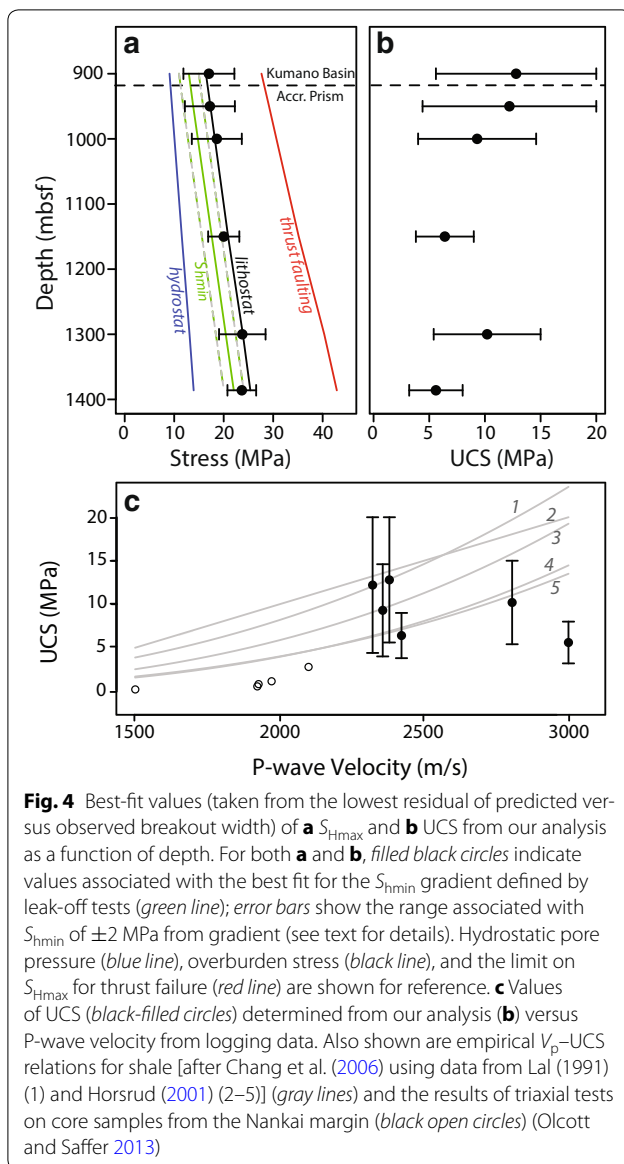


Fig. 4 Best-fit values (taken from the lowest residual of predicted versus observed breakout width) of **a** S_{Hmax} and **b** UCS from our analysis as a function of depth. For both **a** and **b**, filled black circles indicate values associated with the best fit for the S_{Hmin} gradient defined by leak-off tests (green line); error bars show the range associated with S_{Hmin} of ± 2 MPa from gradient (see text for details). Hydrostatic pore pressure (blue line), overburden stress (black line), and the limit on S_{Hmax} for thrust failure (red line) are shown for reference. **c** Values of UCS (black-filled circles) determined from our analysis (**b**) versus P-wave velocity from logging data. Also shown are empirical V_p -UCS relations for shale [after Chang et al. (2006) using data from Lal (1991) (1) and Horsrud (2001) (2–5)] (gray lines) and the results of triaxial tests on core samples from the Nankai margin (black open circles) (Olcott and Saffer 2013)

20.8–26.6 MPa at 1386 mbsf. Predicted values of in situ UCS range from 5.6 to 20 MPa at 900 mbsf to 3.2–8 MPa at 1386 mbsf.

Our results suggest that the in situ stress state lies in a normal to strike-slip faulting regime. This is consistent with a range of independent observations, including widespread recent normal faulting in Kumano basin (e.g., Sacks et al. 2013), and in situ wireline hydraulic fracturing measurements conducted while drilling ~20-km landward (Saffer et al. 2013). Our results also indicate that empirically derived relations commonly used to estimate rock strength from P-wave velocity for shale may slightly overestimate UCS in mudstone and could lead to overestimates of far-field stresses determined from breakout widths.

Authors' contributions

KAH designed the approach to the analysis in the manuscript, ran all models, wrote the first draft, and participated in the Exp. 338 during which much of the data was obtained. DMS and BD were involved in all data collection during Exp. 338 & 314, contributed to the conception of the manuscript, analyzing the data generated in analysis, and provided critical revisions to the text of the manuscript. All authors read and approved the final manuscript.

Author details

¹ Department of Geosciences and Center for Geofluids, Geomechanics, and Geohazards, The Pennsylvania State University, University Park, PA 16802, USA. ² Department of Earth Science, Rice University, Houston, TX 77005, USA.

Acknowledgements

This paper utilizes data from the Integrated Ocean Drilling Program (now the International Ocean Discovery Program), which are publically available via www.IODP.org. We thank Emily Brodsky for discussions that helped significantly with the framing of this paper and the IODP Expedition 338 science party and shipboard crew who obtained and analyzed the data used in this manuscript.

Received: 29 January 2016 Accepted: 14 June 2016

Published online: 19 July 2016

References

- Amadei B, Stephansson O (1997) Rock stress and its measurement. Chapman & Hall, London
- Ando M (1975) Source mechanisms and tectonic significance of historical earthquakes along the Nankai Trough, Japan. *Tectonophysics* 27(2):119–140
- Ashi J, Lallamant S, Masago H, and the Expedition 315 Scientists (2008) NanTroSEIZE Stage 1A: NanTroSEIZE megasplay riser pilot. IODP Prel. Rept. 315
- Ashi J, Lallamant S, Masago H, and the Expedition 315 Scientists (2009) Expedition 315 summary. In: Kinoshita M, Tobin H, Ashi J, Kimura G, Lallamant S, Scream E, Curewitz D, Masago H, Moe KT, and the Expedition 314/315/316 Scientists. *Proceedings of IODP 314/315/316*. Integrated Ocean Drilling Program Management International Inc., Washington, DC
- Bell JS (1990) Investigating stress regimes in sedimentary basins using information from oil industry wireline logs and drilling records. In: Hurst A, Lovell MA, Morton AC (eds) *Geological applications of wireline logs*, vol 48. Geological Society Special Publications, London, pp 305–325
- Boston B, Moore GF, Jurado MJ, Sone H (2016) Deformation of the Nankai Trough inner accretionary prism: the role of inherited structures. *Geochim Geophys Geosyst* 17:485–500
- Brudy M, Zoback MD, Fuchs M, Rummel F, Baumgärtner J (1997) Estimation of the complete stress tensor to 8 km depth in the KTB scientific drill holes: implications for crustal strength. *J Geophys Res* 102(18):453–475
- Byrne TB et al (2009) Anelastic strain recovery reveals extension across SW Japan subduction zone. *Geophys Res Lett* 36(23):L23310
- Chang C, Zoback MD, Khaksar A (2006) Empirical relations between rock strength and physical properties in sedimentary rocks. *J Petrol Sci Eng* 51(3–4):223–237
- Chang C, McNeill L, Moore J, Lin W, Conin M, Yamada Y (2010) In situ stress state in the Nankai accretionary wedge estimated from borehole wall failures. *Geochim Geophys Geosyst* 11(12):Q0AD04
- Engelder T (1993) *Stress regimes in the lithosphere*. Princeton University Press, Princeton
- Expedition 326 Scientists (2011) NanTroSEIZE stage 3: plate boundary deep riser: top hole engineering. ODP Prel. Rept. 326
- Guo J, Underwood MB, Likos WJ, Saffer DM (2013) Apparent overconsolidation of mudstones in the Kumano Basin of southwest Japan: implications for fluid pressure and fluid flow within a forearc setting. *Geochim Geophys Geosyst* 14(4):1023–1038
- Hardebeck JL (2012) Coseismic and postseismic stress rotations due to great subduction zone earthquakes. *Geophys Res Lett* 39(21):L21313
- Henry P, Kanamatsu T, Moe K, and the Expedition 333 Scientists (2012) In: *Proceedings of IODP 333*. Integrated Ocean Drilling Program Management International Inc., Tokyo

- Hill IA, Taira A, Firth JV et al (1993) In: *Proceedings of ODP Science Results*. 131. Ocean Drilling Program, College Station
- Horsrud P (2001) Estimating mechanical properties of shale from empirical correlations. *SPE Drill Complet* 16(2):68–73
- Huffman KH, Saffer DM (2016) In situ stress magnitudes at the toe of the Nankai Trough Accretionary Prism, offshore Shikoku Island, Japan. *J Geophys Res* 121:1202–1217
- Hung JH, Ma KF, Wang CY, Ito H, Lin W, Yeh EC (2009) Subsurface structure, physical properties, fault-zone characteristics and stress state in scientific drill holes of Taiwan Chelungpu Fault Drilling Project. *Tectonophysics* 466(3):307–321
- Ito T, Funato A, Lin W, Doan M-L, Boutt DF, Kano Y, Ito H, Saffer D, McNeill LC, Byrne T, Moe KT (2013) Determination of stress state in deep subsea formation by combination of hydraulic fracturing in situ test and core analysis: a case study in the IODP Expedition 319. *J Geophys Res* 118:1203–1215
- Karig DE, Ingle JC Jr et al (1975) Initial Reports. DSDP 31. U.S. Govt. Printing Office, Washington
- Kerkar P, Hareland G, Fonseca E, Hackbarth C (2014) Estimation of rock compressive strength using downhole weight-on-bit and drilling models. In: *Extended abstracts for international petroleum technology conference*
- Kinoshita M, Tobin H, Ashi J, Kimura G, Lallement S, Screation EJ, Curewitz D, Masago H, Moe KT, and the Expedition 314/315/316 Scientists (2009) In: *Proceedings of IODP, 314/315/316. Integrated Ocean Drilling Program Management International, Inc., Washington, DC*
- Kirsch E (1898) Die theorie der elastizität und die bedürfnisse der festigkeitstheorie. *Zeitschrift des Vereines deutscher Ingenieure* 42:797–807
- Kopf A, Araki E, Toczko S, and the Expedition 332 Scientists (2011) In: *Proceedings of IODP 332. Integrated Ocean Drilling Program Management International, Inc., Tokyo*
- Lal M (1999) Shale stability: drilling fluid interaction and shale strength. In: *SPE Latin American and Caribbean Petroleum Engineering Conference held in Caracas, Venezuela*
- Lin WR, Kwasniewski M, Imamura T et al (2006) Determination of three-dimensional in situ stresses from anelastic strain recovery measurement of cores at great depth. *Tectonophysics* 426(1–2):221–238
- Lin W, Yamamoto K, Ito H, Masago H, Kawamura Y (2008) Estimation of minimum principal stress from an extended leak-off test onboard the Chikyu drilling vessel and suggestions for future test procedures. *Sci Drill* 6:43–47
- Lin W et al (2010) Present-day principal horizontal stress orientations in the Kumano forearc basin of the southwest Japan subduction zone determined from IODP NanTroSEIZE drilling Site C0009. *Geophys Res Lett* 37(13):L13303
- Lin W, Conin M, Moore JC, Chester FM, Nakamura Y, Mori JJ, Anderson L, Brodsky EE, Eguchi N, Expedition 343 Scientists (2013) Stress state in the largest displacement area of the 2011 Tohoku-Oki earthquake. *Science* 339(6120):687–690
- Lin W et al (2015) Distribution of stress state in the Nankai subduction zone, southwest Japan and a comparison with Japan Trench. *Tectonophysics*. doi:10.1016/j.tecto.2015.05.008
- Mikada H, Becker K, Moore JC, Klaus A et al (2002) In: *Proceedings of the ocean drilling program initial reports volume 196. Ocean Drilling Program, College Station*
- Miyazaki S, Heki K (2001) Crustal velocity field of southwest Japan: subduction and arc-arc collision. *J Geophys Res* 106(B3):4305–4326
- Moore GF, Shipley TH, Stoffa PL, Karig DE, Taira A, Kuramoto S, Tokuyama H, Suyehiro K (1990) Structure of the Nankai Trough accretionary zone from multichannel seismic reflection data. *J Geophys Res* 95(B6):8753–8765
- Moore GF, Taira A, Klaus A et al (2001) In: *Proceedings of ODP Initial Reports*. 190. Ocean Drilling Program Scientific Prospectus No. 96. Ocean Drilling Program, College Station
- Moore GF, Park JO, Bangs NL, Gulick SP, Tobin HJ, Nakamura Y, Sato S, Tsuji T, Yoro T, Tanaka H, Uraki S, Kido Y, Sanada Y, Kuramoto S, Taira A (2009) Structural and seismic stratigraphic framework of the NanTroSEIZE Stage 1 transect. In: Kinoshita M, Tobin H, Ashi J, Kimura G, Lallement S, Screation EJ, Curewitz D, Masago H, Moe KT and the Expedition, 314/315/316 Scientists (eds.) *Proceedings of the integrated ocean drilling program 314/315/316*, pp 1–46
- Moore G, Kanagawa K, Strasser M, Dugan B, Maeda L, Toczko S, the Expedition 338 Scientists (2013) NanTroSEIZE Stage 3: NanTroSEIZE plate boundary deep riser 2. *Sci Drill* 17:1–12
- Moos D, Zoback M (1990) Utilization of observations of well bore failure to constrain the orientation and magnitude of crustal stresses: applications to continental, Deep Sea Drilling Project, and Ocean Drilling Program boreholes. *J Geophys Res* 95(B6):9305–9325
- Moran K, Bruckmann W, Feeser V, and Campanella RG (1993) In situ stress conditions at Nankai Trough, Site 808. In: Hill IA, Taira A, Firth JV et al (1993) *Proceedings of ODP, Science Results, 131, Ocean Drilling Program, College Station*, pp 283–291
- Olcott KH, Saffer DM (2013) Laboratory measurements of rock strength: implications for estimating in situ stress from wellbore failures in shallow marine mudstones. In: *Paper presented at the 3rd annual in situ rock stress symposium, Sendai, Japan*
- Peacock S, Westbrook GK, Bais G (2010) S-wave velocities and anisotropy in sediments entering the Nankai subduction zone, offshore Japan. *Geophys J Int* 180(2):743–758
- Sacks A, Saffer DM, Fisher D (2013) Analysis of normal fault populations in the Kumano forearc basin, Nankai Trough, Japan: 2. Principal axes of stress and strain from inversion of fault orientations. *Geochem Geophys Geosyst* 14(6):1973–1988
- Saffer DM, McNeill L, Byrne T, Araki E, Toczko S, Eguchi N, Takahashi K and the Expedition 319 Scientists (2010) In: *Proceedings of IODP 319. Integrated Ocean Drilling Program Management International Inc., Tokyo*
- Saffer DM et al (2013) In situ stress and pore pressure in the Kumano forearc basin, offshore SW Honshu from down-hole measurements during riser drilling. *Geochem Geophys Geosyst* 14(5):1454–1470
- Saito S, Underwood MB, Kubo Y, and the Expedition 322 Scientists (2010) In: *Proceedings of IODP 322. Integrated Ocean Drilling Program Management International Inc., Tokyo*
- Seno T, Stein S, Gripp AE (1993) A model for the motion of the Philippine Sea plate consistent with NUVEL-1 and geological data. *J Geophys Res* 98(B10):17941–17948
- Song I, Saffer DM, Flemings PB (2011) Mechanical characterization of slope sediments: constraints on in situ stress and pore pressure near the tip of the megasplay fault in the Nankai accretionary complex. *Geochem Geophys Geosyst* 12:Q0AD17
- Strasser M, Dugan B, Kanagawa K, Moore GF, Toczko S, Maeda L, and the Expedition 338 Scientists (2014) In: *Proceedings of IODP 338. Integrated Ocean Drilling Program, Yokohama*
- Takeshita T, Yamaguchi A, Shigematsu N (2014) Stress reversal recorded in calcite vein cuttings from the Nankai accretionary prism, southwest Japan. *Earth Planets Space* 66:144. doi:10.1186/s40623-014-0144-4
- Tobin H, Kinoshita M, Ashi J, Lallement S, Kimura G, Screation EJ, Moe KT, Masago H, Curewitz D, and the Expedition 314/315/316 Scientists (2009) NanTroSEIZE Stage 1 expeditions: introduction and synthesis of key results. In: Tobin KH, Ashi J, Kimura G, Lallement S, Screation EJ, Curewitz D, Masago H, Moe KT, and the Expedition 314/315/316 Scientists (eds.) *Proceedings of IODP 314/315/316. Integrated Ocean Drilling Program Management International Inc., Washington, DC*
- Tobin H, Hirose T, Saffer D, Toczko S, Maeda L, Kubo Y, and the Expedition 348 Scientists (2015) In: *Proceedings of IODP, 348. Integrated Ocean Drilling Program, College Station*
- Tsuji T, Dvorkin J, Mavko G, Nakata N, Matsuoka T, Nakanishi A, Kodaira S, Nishizawa O (2011) VP/VS ratio and shear-wave splitting in the Nankai Trough seismogenic zone: insights into effective stress, pore pressure, and sediment consolidation. *Geophysics* 76(3):71
- Wang K, Hu Y (2006) Accretionary prisms in subduction earthquake cycles: the theory of dynamic Coulomb wedge. *J Geophys Res* 111:B06410
- Yamada Y, Shibamura J (2015) Small-scale stress fluctuations in borehole breakouts and their implication in identifying potential active faults around the seismogenic megasplay fault, Nankai Trough, SW Japan. *Earth Planets Space* 67:17. doi:10.1186/s40623-014-0176-9
- Zhou S (1994) A program to model the initial shape and extent of borehole breakout. *Comput Geosci* 20:1143–1160
- Zoback MD (2007) *Reservoir geomechanics*. Cambridge University Press, New York
- Zoback MD, Healy JH (1992) In situ stress measurements to 3.5 km Depth In the Cajon Pass scientific research borehole: implications for the mechanics of crustal faulting. *J Geophys Res* 97:0148–0227